Environ Geochem Health (2025) 47:308
https://doi.org/10.1007/s10653-025-02625-3

ORIGINAL PAPER

Contamination of heavy metal(loid)s in groundwater around mining and smelting area: quantitative source-oriented health risk assessment

Shaobin Shao · Yuan Tang · Chao Wang · Xinyuan Liu · Congqing Wang · Wanjun Wang

Received: 12 March 2025 / Accepted: 20 June 2025 / Published online: 9 July 2025

Abstract The accumulation of heavy metal(loid)s (HMs) in groundwater from mining and smelting industries threatens ecological systems and public health, yet quantitative source-oriented health risks to surrounding residents remain underexplored. This study investigated the pollution characteristics, spatial distribution, source apportionment, and associated health risks of HMs in groundwater at a typical mining-smelting site in China. Sixteen villages near the industrial complex were designated as the exposure area, while three villages 30 km away served as the control area. Fourteen HMs (Mn, Fe, Cu, Zn, Mo, As, Cd, Pb, Sb, V, Cr, Co, Ni, Tl) were detected in the exposure area's groundwater, with a total HM (ΣHMs) mean concentration of 74.07 μg/L—significantly higher than the control area's 37.08 μg/L. Essential HMs (EHMs) dominated the composition, with Zn and Fe as the most abundant elements, whereas non-essential HMs (NEHMs) like Cr and Pb exceeded drinking water standards set by the World Health Organization (WHO) and U.S. Environmental Protection Agency (U.S. EPA). Spatial distribution showed high HM contamination at sites adjacent to the smelting plant. Principal components analysis (PCA) and positive matrix factorization (PMF) models identified mining (34.0%) and smelting (41.3%) as major sources of HMs. Probabilistic health risk assessment via Monte Carlo simulation revealed that 17.9% of adult and 24.7% of child carcinogenic risks in the exposure area exceeded the definite risk threshold value of 10^{-4}, primarily driven by As and Cr ingestion. Source-oriented health risks were assessed by integrating PMF source apportionment into risk model to evaluate the HM risks from identified sources. Results revealed that smelting activities contributed 43.5% (adults) and 43.6% (children) of total carcinogenic risks, while mining accounted for 36.0% in both populations. These findings highlight smelting operations as the primary driver of groundwater HM contamination and emphasize the need for targeted groundwater remediation to mitigate health risks from industrial activities.

Supplementary Information The online version contains supplementary material available at https://doi.org/10.1007/s10653-025-02625-3.

S. Shao · Y. Tang · C. Wang · X. Liu · C. Wang · W. Wang (✉)
Guangdong Key Laboratory of Environmental Catalysis and Health Risk Control, Guangdong Hong Kong-Macao Joint Laboratory for Contaminants Exposure and Health, Institute of Environmental Health and Pollution Control, Guangdong University of Technology, Guangzhou 510006, China
e-mail: wanjun@gdut.edu.cn

S. Shao · Y. Tang · C. Wang · X. Liu · C. Wang · W. Wang
Guangzhou Key Laboratory Environmental Catalysis and Pollution Control, Guangdong Basic Research Center of Excellence for Ecological Security and Green Development, School of Environmental Science and Engineering, Guangdong University of Technology, Guangzhou 510006, China

Keywords Mining and smelting industry · Heavy metal(loid)s · Groundwater · Health risk · Source-oriented health risk assessment

Introduction

Heavy metal(loid)s (HMs), naturally occurring elements in the Earth's crust, are ubiquitously distributed in aquatic environments through both anthropogenic and natural processes (Adnan et al., 2024). While geological activities (e.g., bedrock weathering, and volcanic emissions) contribute to their natural mobilization and enrichment in aquatic environments (Hao et al., 2024), industrial activities—including mining, smelting, electroplating, and electronics manufacturing—have emerged as the dominant contamination sources in recent decades (Burri et al., 2019; Cai et al., 2019). HMs from industrial sectors can enter into groundwater systems through a variety of pathways, such as soil infiltration (Kayastha et al., 2022), and wastewater discharge (Zhang et al., 2023). Among these industries, mining and smelting are two of the world's most critical industries that are associated with HM emissions (Adnan et al., 2024; Jiang et al., 2022). Therefore, it is imperative to study the pollution characteristics, spatial distribution, source apportionment, and health risks of HMs in groundwater at mining and smelting-impacted sites.

The ecological consequences of HM pollution are profound, causing macroinvertebrate mortality and microbial community shifts that degrade aquatic ecosystems (Kahlon et al., 2018; Li et al., 2024). Of greater concern are bioaccumulative HMs (cadmium (Cd), chromium (Cr), lead (Pb), arsenic (As)) that biomagnify through food chains (Kakade et al., 2020; Wang et al., 2023). The International Agency for Research on Cancer (IARC) has classified As, Cd, Cr, and nickel (Ni) as Group-I carcinogens (Podgorski & Berg, 2020), associated with nephrotoxicity, neurodevelopmental disorders, and malignancies (Rehman et al., 2020). Even Group-II carcinogens like Pb demonstrate dose-dependent toxicity, causing neurological, hematological, and reproductive damage (Ayejoto & Egbueri, 2024). The health impacts of HMs exhibit distinct patterns based on their biological roles and chemical properties. Essential heavy metal(loid)s (EHMs) like zinc (Zn) and iron (Fe) serve vital physiological functions at trace levels but demonstrate dose-dependent toxicity when accumulated excessively through industrial discharges (Sanga et al., 2022). Conversely, non-essential heavy metal(loid)s (NEHMs) such as Cd and Cr display inherent hypertoxicity, with chronic exposure linked to cardiovascular dysfunction, developmental disorders, and carcinogenic effects even at minimal concentrations (Eziz et al., 2023). Given their persistence, bioaccumulation potential, and capacity for long-range hydrological transport, HM contamination in groundwater systems has emerged as a critical environmental health concern.

The health risks of HMs in groundwater are conventionally assessed using a framework based on the United States Environmental Protection Agency (U.S. EPA). These health risk assessment approaches typically prove inadequate due to their overreliance on total metal concentrations and static exposure parameters, failing to account for parameter uncertainty. (Sakizadeh & Zhang, 2021; Sheng et al., 2022). Fortunately, as a probabilistic assessment method, Monte Carlo simulation overcomes these limitations by quantifying exposure variability across various scenarios, providing more reliable probabilistic estimates for risk assessments (Eid et al., 2024). The identification and characterization of key human health risk factors is a prerequisite for the effective prevention and control of groundwater contamination (Ganyaglo et al., 2019; Han et al., 2023). Due to the diverse sources of HMs, each source may result in significantly different health risks (Huang et al., 2021; Sun et al., 2022). Therefore, there is an urgent need to clarify the relationship among human health risks, HMs, and the sources, and to develop a source-oriented risk assessment methodology to identify the main sources of health risks. Although the use of receptor models for health risk assessment has become the current mainstream approach, the inability of some models (e.g., principal component analysis (PCA), factor analysis, and cluster analysis) to obtain non-negative results or to deal with process data below the detection level is detrimental to source-oriented assessment (Islam et al., 2019). Many studies have demonstrated that the positive matrix factorization (PMF) model suggested by the U.S. EPA. is a useful tool for overcoming this shortcoming (Guan et al., 2018; Rashid et al., 2023). Therefore, a multidisciplinary approach combining Monte Carlo simulation, PMF models, and health risk assessment

model becomes an important tool for identifying key pollution source and quantifying source-oriented health risks.

This study investigated HM contamination in groundwater from drinking water wells in a residential area (5.5 × 6.5 km) with 16 villages, which are located near mining and smelting plants. Additionally, 3 villages located 30 km away from the expose area without industrial impacts were selected as control area. A multidisciplinary approach, combining geospatial analyses, PCA, PMF model, Monte Carlo simulation-based health risk assessment, and source-oriented health risk assessment, was employed to investigate the pollution characteristics, spatial distribution, source apportionment, and health risks of HMs in groundwater at this mining and smelting-impacted site. Specifically, this study's objectives include: (1) quantifying HM contamination levels and comparing them with international drinking water standards; (2) identifying spatial distribution patterns and contamination sources; (3) evaluating carcinogenic and non-carcinogenic risks for adults and children, with emphasis on exposure pathways and source-specific contributions. This is a comprehensive report on the spatial distribution characteristics and quantitative source-oriented health risk assessment of HMs in groundwater in a complex mining and smelting contaminated region, which can provide valuable data to support groundwater safety protection in industrial contaminated sites.

Materials and methods

Study area and sample sites

The study area is located in Daye City, Hubei Province, a region with a rich history and abundant mineral resources. Daye City is located in the copper-iron polymetallic mineralization belt in the middle and lower reaches of the Yangtze River, and the silica-type deposits are commonly associated with sulfide minerals containing vanadium (V), molybdenum (Mo), and cobalt (Co). These naturally occurring heavy metals are activated during mining activities and become the material basis for groundwater pollution. The city is rich in resources such as copper ore, iron ore, and wollastonite, and the mining and smelting of copper ore and iron ore have spurred the growth of related industries. Groundwater plays a critical role in Daye City's water supply system, serving both life and industrial needs. The aquifer system is predominantly composed of Quaternary unconsolidated deposits and bedrock fissure aquifers. The unconsolidated deposits typically range in thickness from several to tens of meters, while the bedrock fissure aquifers display considerable spatial variability in their thickness distribution. The direction of groundwater flow is controlled by topography and aquifer structure, and generally flows from northwest to southeast. A 5.5 × 6.5 km populated area with both mining and smelting plants was defined as an exposure area, as it was subjected to pollution from mining and smelting operations (Lu et al., 2025). The smelting plant has been in operation since May 2005, and the mining plant has been in operation since December 2004.

Sample collection and instrument analysis

Sixteen villages evenly distributed in the exposure area were selected as sampling sites (R1–R16) for collecting groundwater from drinking water wells. Additionally, 10 sampling sites (C1–C10) in three industrial-free villages located 30 km from the exposure area were designated as control sites (Fig. S1). In the study area, the water depths in all monitoring wells were less than 20 m. For water sampling, two samples were taken at 1.0 m below the surface and three-quarters of the total well depth. These samples were then mixed to obtain the final sample to represent an average of distinct depths of groundwater. Three parallel samples were collected at each sampling site, resulting in a total of 78 samples from 26 locations (48 from the exposure area and 30 from the control area). Samples were stored in 50 mL Teflon centrifuge tubes (CNW, China) after being filtered through 0.45 μm membranes. Nitric acid was added to the collected groundwater samples to lower the pH to < 2, and the samples were stored at 4 °C before being analyzed in the laboratory. Water quality indicators were measured on-site by a multi-parameter analyzer (DZB-718 L, Leici, China).

After being digested by a Microwave Digestion System (MARS6, CEM, USA) and filtered through the 0.45 μm membrane, water samples were analyzed by an inductively coupled plasma mass spectrometry (ICP-MS, Agilent 7900, USA) (Miranda et al.,

2022). Based on previous studies of soil and human urine contamination in this area (Qi et al., 2023; Wu et al., 2025), 14 HMs (Mn, Fe, Cu, Zn, Mo, As, Cd, Pb, Sb, V, Cr, Co, Ni, Tl) were selected for analysis. These HMs were classified as EHMs (Mn, Fe, Cu, Zn, Mo) and NEHMs (As, Cd, Pb, Sb, V, Cr, Co, Ni, Tl) according to the Agency for Toxic Substances and Disease Registry (ATSDR, 2022). The multiple-element calibration standard solution (Mn, Fe, Cu, Zn, Mo, As, Cd, Pb, Sb, V, Cr, Co, Ni, Tl) and the internal standard solution (Sc, In, Bi) were obtained from Agilent (U.S.). Instrument parameter settings are consistent with the previous study (Liu et al., 2025). The total recovery rates of HMs ranged from 84.6 to 109.2% and the limit of detection ranged from 0.011 to 0.076 μg/L. Information on the limit of detection and recovery rates for each HM can be found in Table S1.

Quality assurance and quality control

All glassware and sampling containers were soaked in 10% (v/v) nitric acid for 24 h and purged with ultrapure water (resistivity ≥ 18.25 MΩ cm). HM concentrations were quantified by an internal standard method with an eight-point calibration curve (0.1, 0.5, 1, 10, 50, 100, 250, and 500 μg/L). The correlation coefficients of the calibration curves were both greater than 0.995. Program blanks and quality control samples were required for each batch of 10 samples and blank corrections were applied to all concentrations.

Source analysis

As a multivariate statistical technique, PCA reduces the dimensionality of the data by extracting the principal components of the original data, and facilitates the identification of the main factors affecting the quality of the groundwater, to differentiate the contribution of natural sources and anthropogenic sources to the contamination of HMs (Han et al., 2023). The relative contribution of each source to HM contamination in groundwater is further quantified using the PMF model, which can accurately estimate the proportionate contribution of each source to the HM concentration by mathematically modeling the allocation of the source contribution to the different source types (Sheng et al., 2022). Combining PCA and PMF results provides a comprehensive perspective on the source profile and influence of HM contamination in groundwater, and provides a more scientific basis for water quality protection and pollution control.

Source-oriented health risk assessment

The U.S. EPA-based health risk assessment method was used to quantitatively assess the potential risk of HMs to human health (Wang et al., 2025). Using defined risk assessment may lead to overestimation or underestimation of the actual risk of individual output (Yan et al., 2023), Monte Carlo simulation was introduced to calculate the total risk by linear cumulative superposition (Wang et al., 2024). Two main exposure pathways of ingestion and dermal contact were considered for estimating the health risks in this study. Sequentially, a source-oriented health risk assessment method was developed by combining the PMF model and health risk assessment method. Specifically, the PMF model apportions each HM concentration to different sources and further incorporates these results into the health risk assessment to evaluate the risk to human health posed by HMs from identified sources. Carcinogenic risk (CR) values less than 1.0×10^{-6}, between 1.0×10^{-6} and 1.0×10^{-4}, and greater than 1.0×10^{-4} correspond to negligible, potential, and definite risks, respectively. The calculation methodology is described in detail in Texts S1-S3, and the used parameters of the EPA model can be found in Tables S1, S2.

Data analysis

Microsoft Excel 2016 and IBM SPSS Statistics 24.0 were used for initial data preprocessing and descriptive statistical analyses. Inter-group variability of HM concentrations across distinct surface water bodies was evaluated through one-way analysis of variance (ANOVA) with Tukey's post-hoc test, under parametric assumptions of normality (Shapiro–Wilk test, $W > 0.90$) and homogeneity of variances (Levene's test, $F < 3.32$). Statistical significance was determined at $\alpha = 0.05$ confidence level, with p-values adjusted for multiple comparisons using the Benjamini–Hochberg procedure. Probabilistic health risk assessment was performed through Monte Carlo simulation ($n = 10{,}000$ iterations) using Oracle Crystal Ball 16.0. Geospatial distribution patterns of groundwater HMs

were visualized using ArcGIS 10.8, while multivariate graphical representations were constructed in Origin Pro 2024.

Results and discussion

Contamination of HMs in groundwater

The 14 targeted HMs (Mn, Fe, Cu, Zn, Mo, As, Cd, Pb, Sb, V, Cr, Co, Ni, Tl) were all detected in the study area with a detection rate of 90–100% (Table S3). Total HM concentrations (ΣHMs) in the exposure area (40.83–175.10 μg/L, mean: 74.07 μg/L) were twice as high as those in the control area (9.80–62.66 μg/L, mean: 37.08 μg/L), suggesting that mining and smelting activities significantly contributed to groundwater contamination (Fig. 1a). The average concentration of HMs in the exposure area in this study (74.07 μg/L) was higher than a large Cu-smelter in central China (10.27 μg/L) (Cai et al., 2019), but lower than a multi-mineral resource area in north China (210.55 μg/L) (Jiang et al., 2022) and a chromite mining area in Malakand district of Khyber Pakhtunkhwa province (245.1 mg/L) (Rashid et al., 2023). This indicates that the exposure area in this study is of medium pollution level. Further, the concentration of each HM was compared with that in the drinking water quality standards of China, the U.S. EPA, and the World Health Organization (WHO) (Table S3). The mean concentration of each HM in groundwater of the exposure area was within the quality standards of drinking water in China. However, two HMs (Pb, Cr) in some of the sampling sites exceed the drinking water quality in U.S. EPA or WHO standards. The concentration of Pb in 25.0% of the exposure area exceeded the limit value in the U.S. EPA standard, while the concentration of Cr in 31.2% of the exposure area exceeded the limit value in the WHO standard. In contrast, the concentrations of all the HMs in all the sites of the control area were within the drinking water quality standards of China, the U.S. EPA, and the WHO (Table S4). These results suggest that the groundwater in the exposure area was severely contaminated with HMs as compared with the control area.

The compositional differences between EHMs and NEHMs were further analyzed. The results showed that total concentrations of five EHMs (Zn, Fe, Mo, Cu, Mn) accounted for 84.8% and 91.2% of total ΣHMs in the exposure and control area, respectively. Zn and Fe dominated both areas, contributing 48.9% and 26.0% in the exposure area versus 49.8% and 22.1% in the control area (Fig. 1b), with exposure area concentrations being 2.0–2.4 times higher. In contrast, the total concentrations of nine analyzed NEHMs (As, Cd, Pb, Sb, V, Cr, Co, Ni, Tl) represented only 15.2% (exposure area) and 8.8% (control area) of ΣHMs. However, their concentrations were 0.7–15.6 times higher in the exposure area, with Cr (4.7-fold), Sb (10.4-fold), and Pb (15.6-fold) showing statistically significant elevations ($p < 0.05$). This suggests that residents in the exposure area suffered higher exposure from Cr, Sb, and Pb. Of particular concern, chronic exposure to the elevated Cr, Sb, and Pb levels observed may increase the risks of cardiovascular diseases and childhood obesity (Nasab et al., 2022). While EHMs (particularly Zn and Fe) are dominated by mass concentration, the NEHMs—especially Pb and Cr exceeding regulatory standards—represent more critical health threats requiring immediate policy attention.

Spatial distribution of HMs

The spatial distribution of HMs in groundwater was analyzed using inverse distance interpolation (IDI). The results revealed that the top three contaminated sites for ΣHMs were R4 (175.10 μg/L), R3 (169.74 μg/L), and R16 (118.98 μg/L), which were close to the smelting plant (Fig. 2a). Similarly, ΣEHMs concentrations in groundwater at R4, R3, and R16 ranked among the top three highest, at 157.87 μg/L, 159.50 μg/L, and 105.61 μg/L, respectively (Fig. 2b). These three sampling points are located in the southeast direction of the mine and smelting plant. This is consistent with the direction of groundwater flow in the area (northwest to southeast). In addition, the pH and DO at these three sites were relatively low compared to the other sites (Table S5). Figure 2d–i illustrates the spatial distribution of the top 6 HMs in terms of average concentration. The distributions of Zn, Fe, and Cu were similar to those of ΣHMs and ΣEHMs, and the concentrations of these three HMs decreased with increasing distance from the plant. The presence of HMs may stem from direct infiltration into the groundwater system in conjunction with wastewater

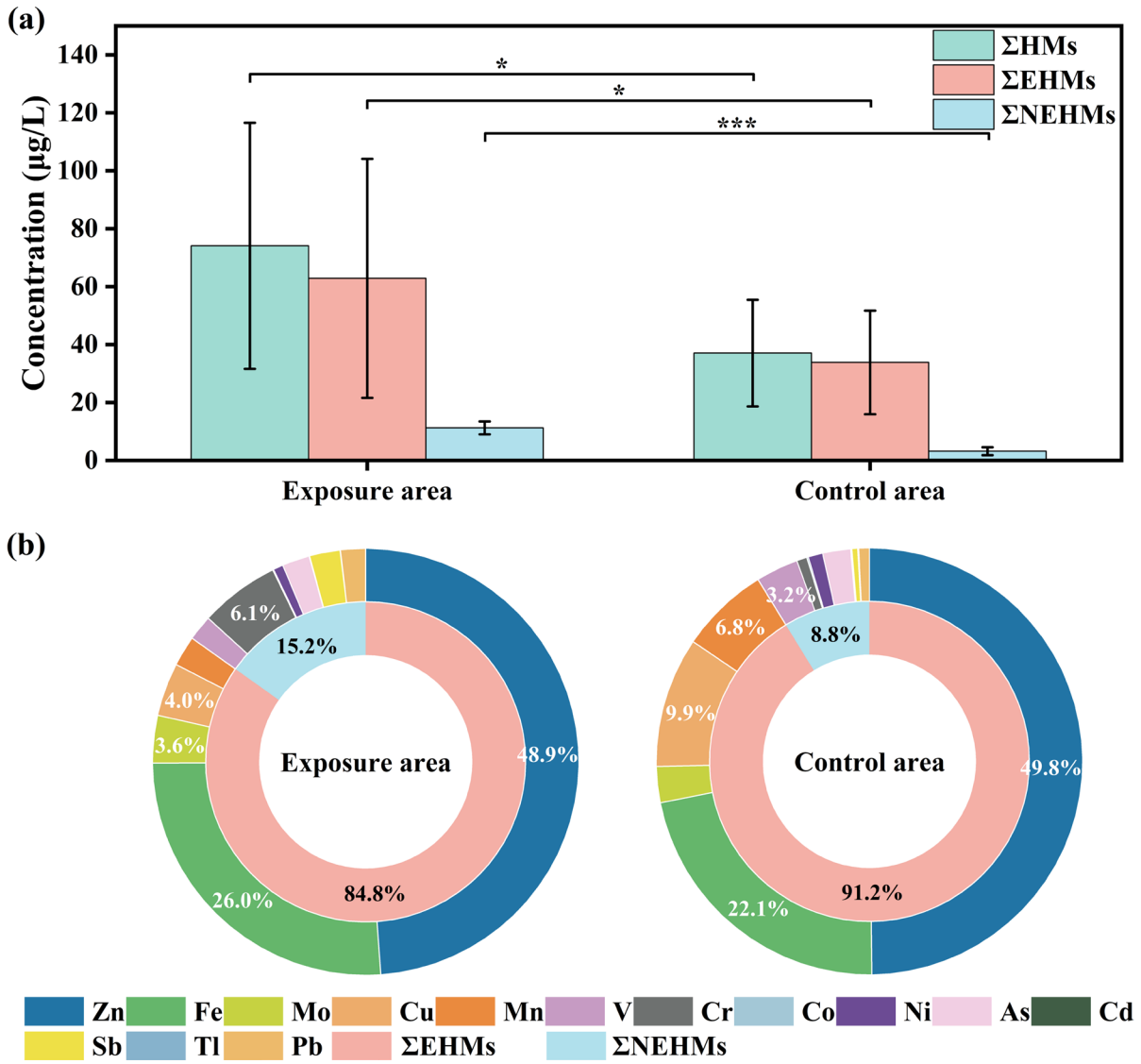

Fig. 1 **a** Concentration of ΣHMs, ΣEHMs, and ΣNEHMs and **b** relative contribution of each HM in the exposure and control areas. ΣHMs is the total concentration of heavy metal(loid)s, ΣEHMs is the total concentration of the essential heavy metal(loid)s (Mn, Fe, Cu, Zn, Mo), and ΣNEHMs is the total concentration of the non-essential heavy metal(loid)s (As, Cd, Pb, Sb, V, Cr, Co, Ni, Tl)

discharges, ore mining, stormwater runoff from open piles, or leaks from underground pipelines (Jafarzadeh et al., 2022). These infiltrated HMs were then transported in the direction of groundwater flow to contaminate the whole area. The contamination of ΣNEHMs in groundwater was mainly concentrated in the southwest direction (Fig. 2c), which is different from the distribution of ΣEHMs. However, the spatial distribution of some NEHMs such as V and Tl was opposite to that of ΣNEHMs, showing a trend of high in the northeast and low in the southwest (Fig. S2). This irregular distribution of HMs suggests that mining and smelting activities may not be the only source of HM contamination in groundwater in the exposure area. Nevertheless, the differences in spatial distribution between different HMs may be related to their specific sources.

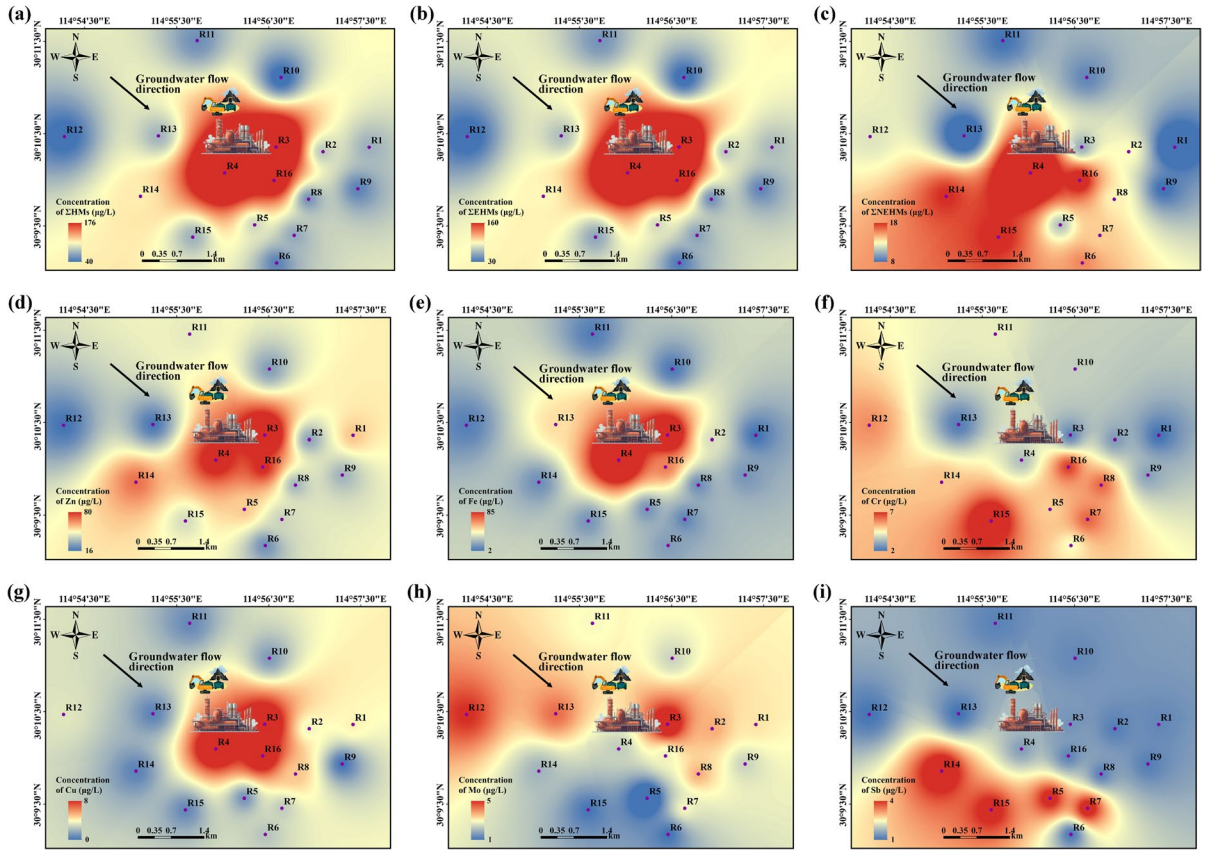

Fig. 2 Spatial distribution of **a** ΣHMs, **b** ΣEHMs, **c** ΣNEHMs, and TOP 6 HMs: **d** Zn, **e** Fe, **f** Cr, **g** Cu, **h** Mo, and **i** Sb in groundwater of the exposure area

Source of HMs in groundwater

The potential sources of HMs were preliminarily evaluated through PCA, which identified key components and factor loadings after dimensionality reduction of groundwater HM data from the exposure area. The analysis demonstrated satisfactory reliability, with a Kaiser–Meyer–Olkin measure of 0.712 (> 0.7 thresholds) and Bartlett's test significance of $p < 0.001$ (Liu et al., 2024). PCA extracted three significant principal components (eigenvalues > 1) that collectively explained 74.5% of the total variance, indicating three probable HM sources in the groundwater (Fig. 3a, Table S6). To quantify source contributions, we subsequently applied the PMF model, which provides superior handling of assessment uncertainties and source identification (Xiang et al., 2024). The PMF analysis similarly resolved three optimal factors, as determined by stabilized Q(True)/Q(Robust) values with increasing factor numbers (Fig. S3). The derived source profiles (Fig. 3c, Tables S7, S8) showed relative contributions of 24.7%, 34.0%, and 41.3% respectively (Fig. 3b).

Factor 1 was characterized by Mn (75.9%) and Sb (55.0%). According to the spatial distribution of Mn and Sb in the study area, both Mn and Sb were distributed in the southwest of the exposure area (Fig. 2i and Fig. S2a), which was far away and less affected by the mining and smelting plants. It has been reported that the variation of Mn in groundwater was mainly controlled by factors such as geomorphology, the depositional environment of the aquifer, and hydraulic properties (Shi et al., 2022). Similarly, some researchers considered that Sb was derived from natural geologic factors (Zhang et al., 2024a). Therefore, combined with field surveys and reported works of literature, factor 1 was considered to be a natural source. Factor 2 was mainly composed of V (75.3%), Mo (72.0%),

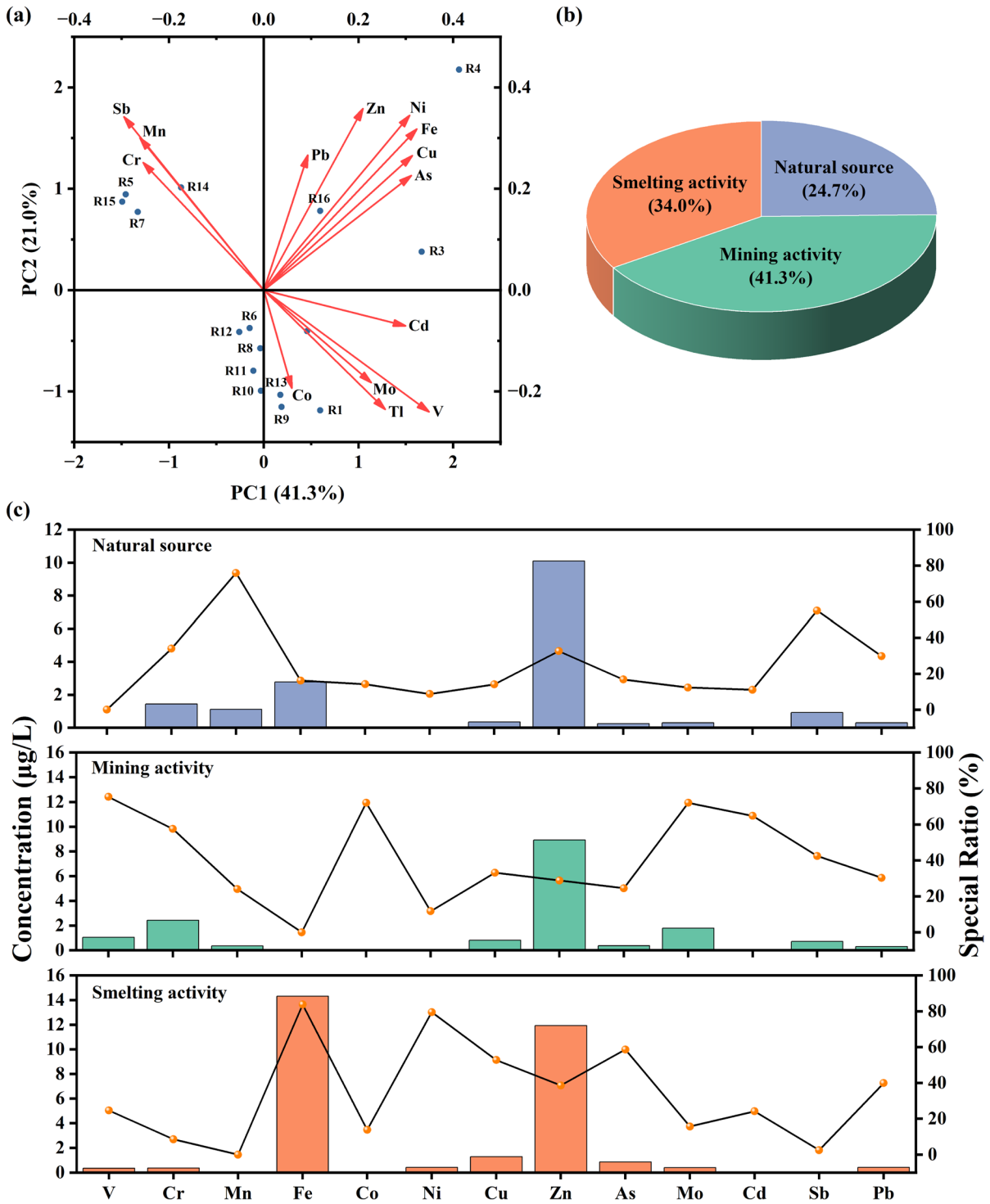

Fig. 3 Source analysis of HMs in groundwater: **a** principal component analysis; **b** three sources identified using the PMF model and their relative contributions; **c** derivation of source profiles and their proportions based on the PMF model. Bars in **c** represent the concentrations of HMs corresponding to each source; curves represent the relative contribution of each source to specific HM

Co (72.0%) and Cd (64.7%). Studies have shown that high concentrations of V and Mo in groundwater typically occur in groundwater surrounding mining areas (Chelnokov et al., 2024; Meng et al., 2018). In addition, it was demonstrated that Co is a major constituent of rock minerals (Rao et al., 2021). Cd has also been shown to be widely present in mining wastewater (Zhang et al., 2024b). The study area is located in the copper-iron polymetallic mineralization belt in the middle and lower reaches of the Yangtze River, and the silica-type deposits are commonly associated with sulfide minerals containing V, Mo, and Co. These naturally occurring heavy metals are activated during mining activities and become the material basis for groundwater pollution. Therefore, according to the field survey of the study area, factor 2 was regarded as a source of mining activity. Factor 3 was dominated by Fe (83.8%), Ni (79.5%), As (58.6%) and Cu (52.7%). Our previous studies of HMs in the wastewater treatment plant and receiving river at this smelting plant found that As, Ni, and Cu are the main HMs in both the wastewater from this smelting plant and the receiving river (Liu et al., 2025), suggesting that Factor 3 may be related to smelting emissions. Meanwhile, it has been shown that Fe in groundwater in industrial parks, especially in areas involved in mining and smelting, is mainly derived from industrial wastewater discharges (Jiang et al., 2021). Therefore, it is inferred that factor 3 was derived from smelting activity. In conclusion, HMs in groundwater in the exposure area were attributed to three sources: natural source, mining activity, and smelting activity. The total relative contribution of mining and smelting activities reached 75.3%, revealing that mining and smelting activities in the area increased HM contamination of the surrounding groundwater.

Probabilistic health risk assessment

Concentration-oriented health risk assessment

In this study, the health risks for adults and children were assessed by Monte Carlo simulations calculating ingestion and dermal exposure pathways to shallow groundwater containing HMs in the study area. The health risks in the exposure area and control area were compared. As shown in Table S9, in the control area, the total carcinogenic risk (TCR) for adults and children were 1.2×10^{-8}–5.8×10^{-4} (mean value: 2.6×10^{-5}) and 5.6×10^{-9}–4.1×10^{-4} (mean value: 2.9×10^{-5}) respectively. In the exposure area, the TCR for adults was 4.5×10^{-9}–8.0×10^{-4} (mean value: 6.2×10^{-5}), and for children was 3.7×10^{-8}–6.4×10^{-4} (mean value: 7.1×10^{-5}). The findings suggest that children face higher cancer risks than adults. This elevated risk may be attributed to children's lower body weight (BW) and longer average exposure time (AT) during critical developmental stages (Ashayeri & Keshavarzi, 2019). Notably, the mean TCRs for both adults and children in the exposure area were 2.4-fold higher than those in the control area, indicating that residents in the exposure area are subjected to greater carcinogenic risks from mining and smelting operations. Figure 4a demonstrates the probability distributions of the TCR for adults and children in the exposure and control areas. In the exposure area, 17.9% and 24.7% of carcinogenic risks for adults and children, respectively, exceeded the definite risk threshold of 10^{-4}. By contrast, only 1.4% and 1.5% of risks in the control area exceeded this value, confirming that adults and children in the exposure area face significant carcinogenic risks from mining and smelting activities.

For non-carcinogenic risk assessment, the HI values for both adults and children were below the safety threshold (HI < 1) in both exposure and control areas (Fig. 4b). The calculated HI ranges were 5.0×10^{-6} to 8.6×10^{-1} (adults) and 3.5×10^{-5} to 5.4×10^{-1} (children) in the exposure area, compared to 7.6×10^{-6} to 4.1×10^{-1} (adults) and 4.6×10^{-6} to 2.9×10^{-1} (children) in the control area. Notably, the mean HI values in the exposure area were 3.3 times higher than those in the control area, indicating elevated (though still acceptable) non-carcinogenic risks. These findings align with previous studies in similar environments. Zhao et al. (2023) reported acceptable non-carcinogenic risks (HI < 1) from five HMs (Cr, Cd, Pb, As, and Hg) in groundwater from China's Inner Mongolia mining region, despite finding definite carcinogenic risks ($>10^{-4}$). Similarly, Jiang et al. (2022) found negligible non-carcinogenic risks but significant carcinogenic risks ($>10^{-4}$ for 94% of the population) from seven HMs (As, Hg, Cd, Cr, Pb, Cu, Ni) in northwestern China's multi-mineral resource area. The consistent pattern across studies suggests that while mining and smelting activities may not induce immediate non-carcinogenic health effects, they significantly increase carcinogenic risks. This

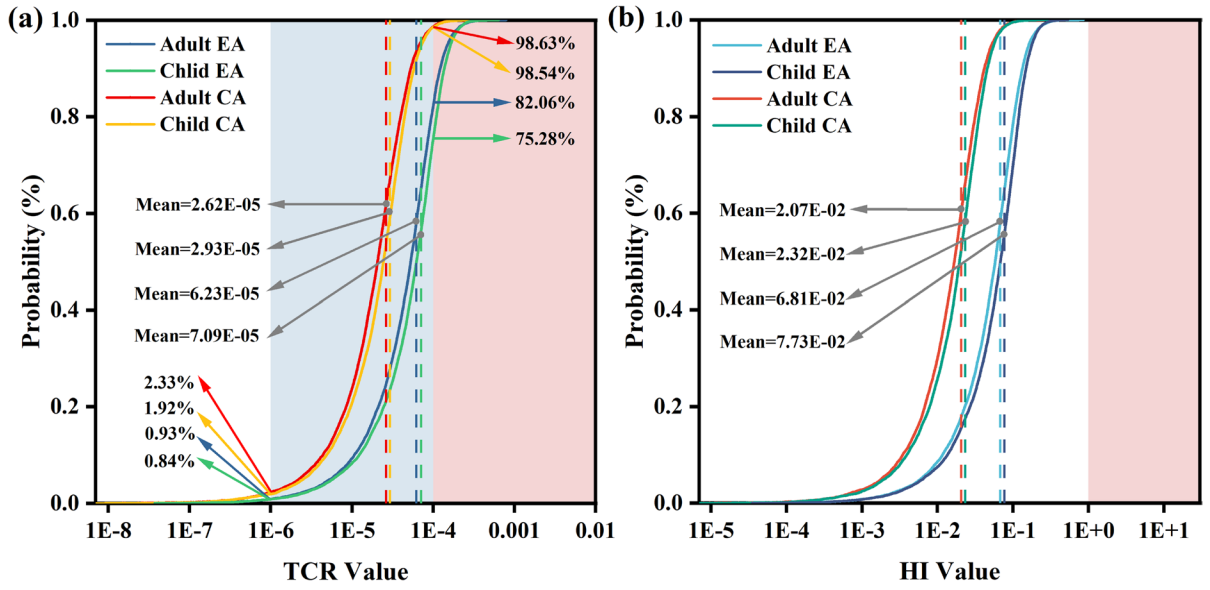

Fig. 4 Cumulative probabilistic estimate of **a** TCR and **b** HI in groundwater. EA is the exposure area. CA is the control area. The white, blue, and red areas in **a** represent negligible risk ($TCR < 10^{-6}$), possible risk ($10^{-6} < TCR < 10^{-4}$), and definite risk ($TCR > 10^{-4}$) in carcinogenic risk, respectively. The white and red areas in **b** represent negligible risk ($HI < 1$) and definite risk ($HI > 1$) in non-carcinogenic risk

discrepancy likely stems from the presence of highly toxic carcinogenic metals, particularly As, which typically dominates the total risk profile at such sites due to its extreme toxicity and prevalence in mineral processing operations.

Comparison of exposure pathways

A comparative assessment of health risks was conducted for adults and children in both exposure and control areas through ingestion and dermal exposure pathways, with results tabulated in Table S10. In the exposure area, adults exhibited carcinogenic risks through ingestion exposure ranging from 1.5×10^{-8} to 5.3×10^{-4} (mean value: 6.1×10^{-5}), whereas dermal exposure demonstrated substantially lower risks (range: 9.9×10^{-11} to 5.3×10^{-6}; mean: 4.5×10^{-7}). This represents a 136-fold greater risk through ingestion compared to dermal exposure. The result of children showed an even more pronounced disparity, with ingestion-associated risks exceeding dermal exposure by factors of 393. Notably, A similar disparity between the two exposure routes was observed in both adults and children in the control area. For non-carcinogenic risks, the HI associated with the ingestion exposure pathway was 156 times higher for adults and 449 times higher for children compared to the dermal exposure pathway. These findings suggest that HMs in groundwater in both exposure and control areas may pose potential health risks primarily through the ingestion exposure pathway.

Contribution of individual HM to total health risks

In terms of carcinogenic risk for individual HM, the carcinogenic risks of V, As, Cr, Mo, Ni, and Sb in the exposure area groundwater exceeded the negligible threshold (10^{-6}) for both adults and children (Fig. 5a, b). And the carcinogenic risks of Cd and Pb were both less than 10^{-6}. The eight HMs produced the same trend of carcinogenic risks to adults and children, with an overall order of: As > Cr > Ni > Mo > Sb > V > Pb > Cd. As and Cr were the main contributors to the carcinogenic risk, with relative contributions of 55.3% and 21.8% for adults, and 55.5% and 21.7% for children, respectively. Notably, all seven HMs except Mo are NEHMs. The high toxicity of these three HMs results in a higher carcinogenic risk, even though the mean concentration of Mo is 1.7 and 4.8 times higher than that of As and Ni, respectively.

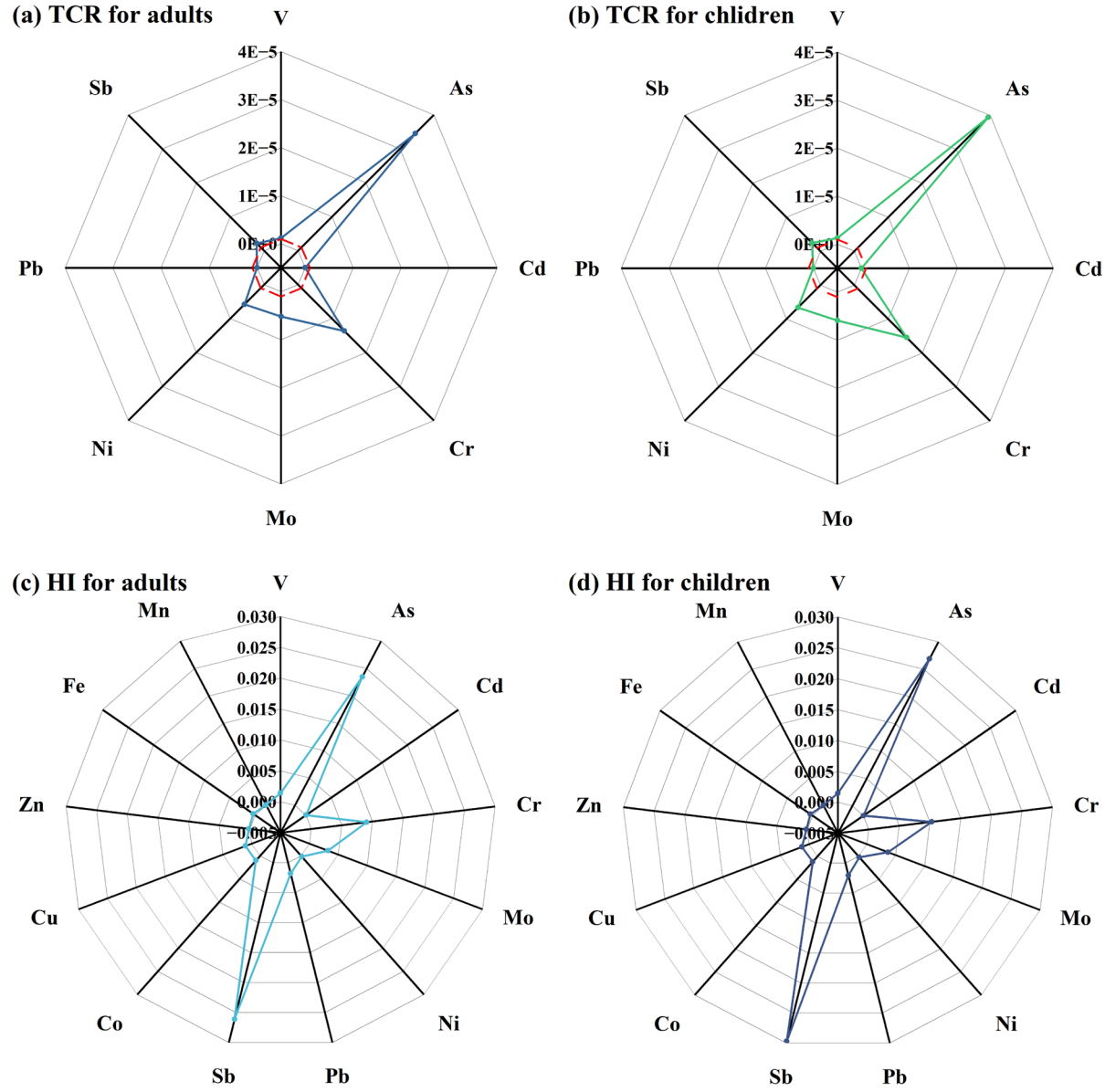

Fig. 5 Star plots for the TCR and HI for **a** and **c** adults, and **b** and **d** children from individual HM. The red lines in **a** and **b** represent the TCR = 10^{-6}

Unexpectedly, Mo, an essential element for humans, also posed a carcinogenic risk above the negligible threshold (10^{-6}), suggesting that even HMs that are essential to humans can pose a cancer risk at high levels.

For non-carcinogenic risks, the HQs of the 13 HMs were all less than the risk threshold (HQ = 1) (Fig. 5c, d), indicating that individual HM posed negligible non-carcinogenic risks to adults and children. In contrast to the order of carcinogenic risk, the magnitude of non-carcinogenic risk posed by the 13 HMs to adults and children was in the order of Sb > As > Cr > Mo > Pb > V > Cu > Co > Fe > Ni > Zn > Mn > Cd. As the major contributors to non-carcinogenic risk, the relative contributions of Sb and As to the HI of adults and children were 38.4%, 34.6%, and 38.3%, 34.7%, respectively. Although the non-carcinogenic risks can be

disregarded, the high contribution rates of As and Sb may imply long-term exposure risks.

Source-oriented health risk assessment

Compared to concentration-oriented health risk assessment, source-oriented health risk assessment can quantify the health risks associated with different sources of HMs and can provide critical data support for risk control at the source (Han et al., 2023). For carcinogenic risk, among the various sources, the carcinogenic risk of HMs for adults was smelting activity (2.71×10^{-5}) > mining activity (2.25×10^{-5}) > natural source (1.28×10^{-5}). The carcinogenic risk for children followed the same order: smelting activity (3.09×10^{-5}) > mining activity (2.55×10^{-5}) > natural source (1.45×10^{-5}) (Fig. 6a). This indicates that smelting activity was the main contributor to the risk of cancer in adults and children in the exposure area. The carcinogenic risk for adults and children due to smelting activity was 2.11 and 2.13 times higher than that from natural sources, accounting for 43.5% and 43.6% of the total carcinogenic risk, respectively (Fig. 6b, d). Altogether, this evidence reveals that smelting activity was the main source of carcinogenic risk for adults and children in the exposure area. It is important to note that the cancer risk from natural source exceeded 10^{-6} for both adults and children, indicating that HMs in groundwater in the exposure area pose a possible carcinogenic risk to human and

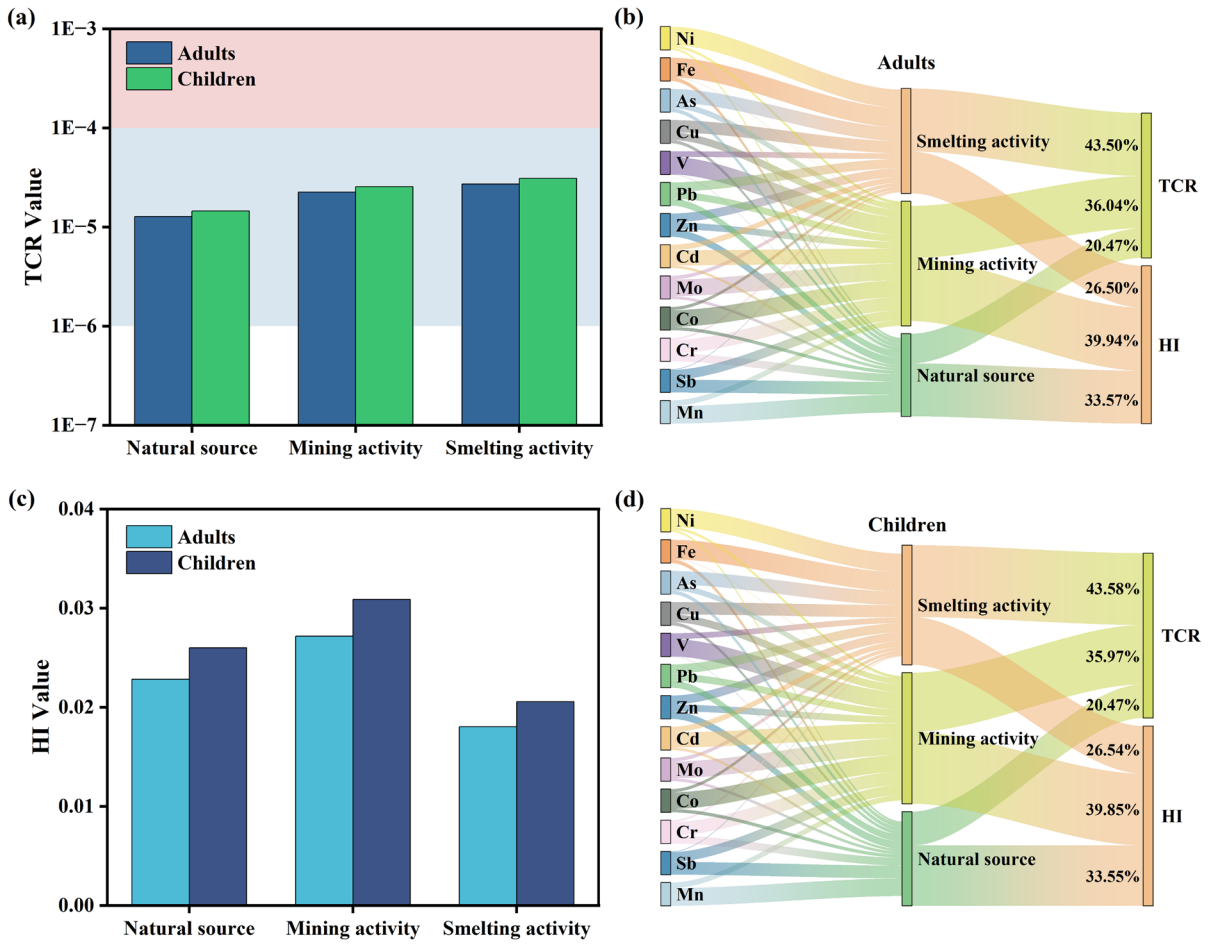

Fig. 6 Source-oriented health risk assessment for **a** TCR and **b** relative contribution of different sources to health risk for adults; **c** HI and **d** relative contribution of different sources to the health risk for children. The white, blue, and red areas in **a** represent negligible risk (TCR < 10^{-6}), possible risk (10^{-6} < TCR < 10^{-4}), and definite risk (TCR > 10^{-4}) in carcinogenic risk, respectively

that groundwater needs to be treated before it can be made available for human consumption.

For non-carcinogenic risks, the HI for adults from different sources were mining activity (2.72×10^{-2}) > natural source (2.28×10^{-2}) > smelting activity (1.80×10^{-2}), and for children were mining activity (3.09×10^{-2}) > natural source (2.60×10^{-2}) > smelting activity (2.06×10^{-2}) (Fig. 6c). The non-carcinogenic risks for both adults and children from different sources were within the normal range for all sample sites (HI < 1), demonstrating that none of the three sources of HM contamination in groundwater posed non-carcinogenic risks to adults and children. In summary, smelting activity was the largest contributor to human carcinogenic risk, while mining source was the largest contributor to non-carcinogenic risk.

The reasons for this result lie in the different industrial processes and characteristic HMs of mining and smelting activity. The mining activity mainly releases HMs from the ore through physical crushing and milling processes. Most of these HMs are presented in the tailings as insoluble minerals (e.g., sulfides, oxides) and have a limited ability to migrate to groundwater. Moreover, mining activity in this study area mainly brings HMs pollution caused by V, Mo, Co, and Cd, which have a low carcinogenic slope factor (SF). However, these metals have low non-carcinogenic reference dose (RfD) values ($RfD_{(V)}=0.007$, $RfD_{(Mo)}=0.005$, $RfD_{(Co)}=0.0003$, $RfD_{(Cd)}=0.0005$, Table S1), resulting in a high non-carcinogenic risk. Smelting activity refines HMs in ores into soluble compounds with high SF by using high-temperature pyro-processes or wet processes with strong acids or bases. For instance, the SF of arsenic (As) is 3.66 as presented in Table S1. This process results in the creation of high concentrations of HMs residues in wastewater and sludges. These residues are more readily transported to groundwater, leading to a high carcinogenic risk. Therefore, smelting activity caused higher carcinogenic risk than mining activity. Priority control should be paid to the smelting activity for mitigating the health risks from HMs in groundwater to the residents in the exposure area.

Uncertainty and sensitivity analysis

There were a few uncertainties in human health risk assessment. First, due to the lack of toxicological data on some of the HMs, the assessment relied on a number of assumptions, which can introduce uncertainty in the assessment (Askari et al., 2024). Second, exposure to different compounds was assumed to be independent in Monte Carlo simulations; however, in practice, some HMs may enter the human body from the same source or through similar exposure pathways, which may lead to inaccurate risk estimates (Jiang et al., 2021). In addition, the uncertainty was further increased by the complexity of the exposure pathways of HMs. Additionally, the parameter values used in the assessment were directly taken from the U.S. EPA's recommended values, which may not be entirely applicable to populations in different countries (Eid et al., 2024). As a result, there is a need to develop alternative assessment frameworks tailored to local contexts in future studies.

The sensitivity of the variables relating to adults and children to TCR and HI was analyzed using Monte Carlo simulation (Bhat et al., 2024). Taking the exposure area as an example, exposure duration (ED) had the greatest impact on the total variance of TCR, accounting for 84.2% and 87.4% in adults and children, respectively (Fig. S5a, b). HM concentrations had the next largest effect on TCR variance, contributing 34.7% in adults and 33.4% in children, followed by daily ingestion rate (IR), which contributed 24.9% in adults and 27.8% in children. In terms of non-carcinogenic risk, ED, exposure frequency (EF) and IR were the top three parameters in terms of relative contribution. The relative contributions of ED, IR, and EF were 84.7%, 25.2%, and 16.9% in adults, and 87.7%, 28.1%, and 18.0% in children, respectively (Fig. S5c, d). In contrast, the large negative contributions of BW to TCR and HI in both adults (− 27.5%, − 27.6%) and children (− 10.2%, − 10.4%) may explain why children were at higher health risks compared to adults.

Conclusion

This study comprehensively investigated the contamination characteristics, spatial distribution, source apportionment, and associated health risks of HMs in groundwater within a mining and smelting-impacted region. The results revealed significant HM contamination in the exposure area, with the mean concentration of ΣHMs (74.07 μg/L) doubling that of the

control area (37.08 µg/L). Concentrations of Cr and Pb exceeded U.S. EPA and WHO standards, highlighting severe anthropogenic contamination. Spatial analysis identified elevated HM levels near the smelting plant (sites R3, R4, R16), associated with groundwater flow direction, suggesting direct infiltration from industrial activities. Conversely, irregular distributions of certain NEHMs (e.g., V, Tl) implied contributions from non-industrial sources. PCA—PMF source apportionment attributed HM contamination to natural processes (24.7%), mining (34.0%), and smelting (41.3%). Smelting activity was identified as the dominant contributor to carcinogenic risk, while mining activity posed the highest non-carcinogenic risk. Probabilistic health risk assessments demonstrated that 17.9% and 24.7% of carcinogenic risks for adults and children in the exposure area exceeded the acceptable carcinogenic risk threshold ($TCR > 10^{-4}$), primarily driven by ingestion of As and Cr. Non-carcinogenic risks, though below thresholds, were elevated in the exposure area, with Sb and As as key contributors. Sensitivity analysis underscored exposure duration and HM concentrations as critical variables influencing risk outcomes. These findings emphasize the urgent need for targeted mitigation strategies, particularly to address smelting-derived emissions and groundwater treatment for Cr and Pb. The results provided the first insight into the quantitative source-oriented health risks of HMs in groundwater from mining and smelting contaminated sites, which helps to formulate pollution control policies for the relevant industries.

Author contributions Shaobin Shao: Investigation, Formal analysis, Data curation, Writing—original draft. Yuan Tang: Methodology, Formal analysis. Chao Wang: Investigation, Visualization. Xinyuan Liu: Formal analysis, Validation. Congqing Wang: Software, Resources. Wanjun Wang: Conceptualization, Funding acquisition, Project administration, Writing—review & editing. All authors have read and agree to their specific contribution.

Funding This work was supported by National Natural Science Foundation of China (42377365, 42122056), Guangdong Basic and Applied Basic Research Foundation (2021B1515020063, 2022A1515010815), National Key Research and Development Program of China (2021YFC1808901), and Guangdong Provincial Key R&D Program (2022-GDUT-A0007).

Data availability No datasets were generated or analysed during the current study.

Declarations

Conflict of interest The authors declare no competing interests.

References

Adnan, M., Xiao, B. H., Ali, M. U., Xiao, P. W., Zhao, P., Wang, H. Y., & Bibi, S. (2024). Heavy metals pollution from smelting activities: A threat to soil and groundwater. *Ecotoxicology and Environmental Safety, 274*, 116189. https://doi.org/10.1016/j.ecoenv.2024.116189

Ashayeri, Y. N., & Keshavarzi, B. (2019). Geochemical characteristics, partitioning, quantitative source apportionment, and ecological and health risk of heavy metals in sediments and water: A case study in Shadegan Wetland, Iran. *Marine Pollution Bulletin, 149*, 110495. https://doi.org/10.1016/j.marpolbul.2019.110495

Askari, M., Soleimani, H., Babakrpur Nalosi, K., Saeedi, R., Abolli, S., Ghani, M., Abtahi, M., & Alimohammadi, M. (2024). Bottled water safety evaluation: A comprehensive health risk assessment of oral exposure to heavy metals through deterministic and probabilistic approaches by Monte Carlo simulation. *Food and Chemical Toxicology, 185*, 114492. https://doi.org/10.1016/j.fct.2024.114492

ATSDR, (2022). Substance Priority List. Agency for toxic substances and disease registry. US Department of Health and Human Services Public Health Ser- vice Atlanta, GA (2023).

Ayejoto, D. A., & Egbueri, J. C. (2024). Human health risk assessment of nitrate and heavy metals in urban groundwater in Southeast Nigeria. *Ecological Frontiers, 44*, 60–72. https://doi.org/10.1016/j.chnaes.2023.06.008

Bhat, M. A., Fan, D. D., Nisa, F. U., Dar, T., Kumar, A., Sun, Q. Q., Li, S. L., & Mir, R. R. (2024). Trace elements in the Upper Indus River Basin (UIRB) of Western Himalayas: Quantification, sources modeling, and impacts. *Journal of Hazardous Materials, 476*, 135073. https://doi.org/10.1016/j.jhazmat.2024.135073

Burri, N. M., Weatherl, R., Moeck, C., & Schirmer, M. (2019). A review of threats to groundwater quality in the anthropocene. *Science of the Total Environment, 684*, 136–154. https://doi.org/10.1016/j.scitotenv.2019.05.236

Cai, L. M., Wang, Q. S., Luo, J., Chen, L. G., Zhu, R. L., Wang, S., & Tang, C. H. (2019). Heavy metal contamination and health risk assessment for children near a large Cu-smelter in central China. *Science of the Total Environment, 650*, 725–733. https://doi.org/10.1016/j.scitotenv.2018.09.081

Chelnokov, G., Lavrushin, V., Ermakov, A., Guo, Q. H., Aidarkozhina, A., Kharitonova, N., Bragin, I., & Pavlov, A. (2024). Toxic element contamination sources in the surface and groundwater of the Elbrus Region: Geochemistry and health risks. *Water, 16*, 701. https://doi.org/10.3390/w16050701

Eid, M. H., Eissa, M., Mohamed, E. A., Ramadan, H. S., Tamás, M., Kovács, A., & Szűcs, P. (2024). New approach into human health risk assessment associated with heavy metals in surface water and groundwater using Monte

Carlo Method. *Science and Reports, 14*, 1008. https://doi.org/10.1038/s41598-023-50000-y

Eziz, M., Sidikjan, N., Zhong, Q., Rixit, A., & Li, X. G. (2023). Distribution, pollution levels, and health risk assessment of heavy metals in groundwater in the main pepper production area of China. *Open Geosci., 15*, 20220491. https://doi.org/10.1515/geo-2022-0491

Ganyaglo, S. Y., Gibrilla, A., Teye, E. M., Owusu-Ansah, E. D. G. J., Tettey, S., Diabene, P. Y., & Asimah, S. (2019). Groundwater fluoride contamination and probabilistic health risk assessment in fluoride endemic areas of the Upper East Region, Ghana. *Chemosphere, 233*, 862–872. https://doi.org/10.1016/j.chemosphere.2019.05.276

Guan, Q. Y., Wang, F. F., Xu, C. Q., Pan, N. H., Lin, J. K., Zhao, R., Yang, Y. Y., & Luo, H. P. (2018). Source apportionment of heavy metals in agricultural soil based on PMF: A case study in Hexi Corridor, northwest China. *Chemosphere, 193*, 189–197. https://doi.org/10.1016/j.chemosphere.2017.10.151

Han, W. J., Pan, Y. J., Welsch, E., Liu, X. R., Li, J. R., Xu, S. S., Peng, H. X., Wang, F. T., Li, X., Shi, H. H., Chen, W., & Huang, C. S. (2023). Prioritization of control factors for heavy metals in groundwater based on a source-oriented health risk assessment model. *Ecotoxicology and Environmental Safety, 267*, 115642. https://doi.org/10.1016/j.ecoenv.2023.115642

Hao, X., Ouyang, W., Gu, X., He, M. C., & Lin, C. Y. (2024). Accelerated export and transportation of heavy metals in watersheds under high geological backgrounds. *Journal of Hazardous Materials, 465*, 133514. https://doi.org/10.1016/j.jhazmat.2024.133514

Huang, J. L., Wu, Y. Y., Sun, J. X., Li, X., Geng, X. L., Zhao, M. L., Sun, T., & Fan, Z. Q. (2021). Health risk assessment of heavy metal(loid)s in park soils of the largest megacity in China by using Monte Carlo simulation coupled with Positive matrix factorization model. *Journal of Hazardous Materials, 415*, 125629. https://doi.org/10.1016/j.jhazmat.2021.125629

Islam, A. R. M. T., Bodrud-Doza, M., Rahman, M. S., Amin, S. B., Chu, R. H., & Al Mamun, H. (2019). Sources of trace elements identification in drinking water of Rangpur district, Bangladesh and their potential health risk following multivariate techniques and Monte-Carlo simulation. *Groundwater for Sustainable Development, 9*, 100275. https://doi.org/10.1016/j.gsd.2019.100275

Jafarzadeh, N., Heidari, K., Meshkinian, A., Kamani, H., Mohammadi, A. A., & Conti, G. O. (2022). Non-carcinogenic risk assessment of exposure to heavy metals in underground water resources in Saraven, Iran: Spatial distribution, monte-carlo simulation, sensitive analysis. *Environmental Research, 204*, 112002. https://doi.org/10.1016/j.envres.2021.112002

Jiang, C. L., Zhao, Q., Zheng, L. G., Chen, X., Li, C., & Ren, M. X. (2021). Distribution, source and health risk assessment based on the Monte Carlo method of heavy metals in shallow groundwater in an area affected by mining activities. *China. Ecotoxicol. Environ. Saf., 224*, 112679. https://doi.org/10.1016/j.ecoenv.2021.112679

Jiang, W. J., Liu, H. W., Sheng, Y. Z., Ma, Z., Zhang, J., Liu, F. T., Chen, S. M., Meng, Q. H., & Bai, Y. N. (2022). Distribution, Source Apportionment, and Health Risk Assessment of Heavy Metals in Groundwater in a Multi-mineral Resource Area, North China. *Exposure and Health, 14*, 807–827. https://doi.org/10.1007/s12403-021-00455-z

Kahlon, S. K., Sharma, G., Julka, J. M., Kumar, A., Sharma, S., & Stadler, F. J. (2018). Impact of heavy metals and nanoparticles on aquatic biota. *Environmental Chemistry Letters, 16*, 919–946. https://doi.org/10.1007/s10311-018-0737-4

Kakade, A., Salama, E. S., Pengya, F., Liu, P., & Li, X. K. (2020). Long-term exposure of high concentration heavy metals induced toxicity, fatality, and gut microbial dysbiosis in common carp. *Cyprinus Carpio. Environ. Pollut., 266*, 115293. https://doi.org/10.1016/j.envpol.2020.115293

Kayastha, V., Patel, J., Kathrani, N., Varjani, S., Bilal, M., Show, P. L., Kim, S. H., Bontempi, E., Bhatia, S. K., & Bui, X. T. (2022). New Insights in factors affecting ground water quality with focus on health risk assessment and remediation techniques. *Environmental Research, 212*, 113171. https://doi.org/10.1016/j.envres.2022.113171

Li, D., Ding, Y., Zhang, Y., Zhang, X. Y., Feng, L. Y., & Zhang, Y. L. (2024). Heavy metals in a typical industrial area-groundwater system: Spatial distribution, microbial response and ecological risk. *Chemosphere, 360*, 142339. https://doi.org/10.1016/j.chemosphere.2024.142339

Liu, S. Z., Wu, K. X., Yao, L., Li, Y. H., Chen, R. N., Zhang, L. P., Wu, Z. B., & Zhou, Q. H. (2024). Characteristics and correlation analysis of heavy metal distribution in China's freshwater aquaculture pond sediments. *Science of the Total Environment, 931*, 172909. https://doi.org/10.1016/j.scitotenv.2024.172909

Liu, X. Y., Wang, C., Wang, W. J., Qiu, Y., Tang, Y., Wang, C. Q., Li, H. L., Li, G. Y., & An, T. C. (2025). Combined pollution of heavy metals and polycyclic aromatic hydrocarbons in non-ferrous metal smelting wastewater treatment plant: Distribution profiles, removal efficiency, and ecological risks to receiving river. *Journal of Hazardous Materials, 486*, 137118. https://doi.org/10.1016/j.jhazmat.2025.137118

Lu, P., He, R. J., Wu, Y. J., Wu, B. Z., Li, H. L., He, C., Lin, M. Q., Wang, M. M., Cai, W. W., Shen, X. T., Li, G. Y., Cao, Z. G., & An, T. C. (2025). Urinary metabolic alterations associated with occupational exposure to metals and polycyclic aromatic hydrocarbons based on non-target metabolomics. *Journal of Hazardous Materials, 487*, 137158. https://doi.org/10.1016/j.jhazmat.2025.137158

Meng, R. H., Chen, T., Zhang, Y. X., Lu, W. J., Liu, Y. T., Lu, T. C., Liu, Y. J., & Wang, H. T. (2018). Development, modification, and application of low-cost and available biochar derived from corn straw for the removal of vanadium(v) from aqueous solution and real contaminated groundwater. *RSC Advances, 8*, 21480–21494. https://doi.org/10.1039/c8ra02172d

Miranda, L. S., Ayoko, G. A., Egodawatta, P., & Goonetilleke, A. (2022). Adsorption-desorption behavior of heavy metals in aquatic environments: Influence of sediment, water and metal ionic properties. *Journal of Hazardous Materials, 421*, 126743. https://doi.org/10.1016/j.jhazmat.2021.126743

Nasab, H., Rajabi, S., Eghbalian, M., Malakootian, M., Hashemi, M., & Mahmoudi-Moghaddam, H. (2022). Association of As, Pb, Cr, and Zn urinary heavy metals levels with predictive indicators of cardiovascular disease and obesity in children and adolescents. *Chemosphere, 294*, 133664. https://doi.org/10.1016/j.chemosphere.2022.133664

Podgorski, J., & Berg, M. (2020). Global threat of arsenic in groundwater. *Science, 368*, 845–850. https://doi.org/10.1126/science.aba1510

Qi, M. D., Wu, Y. J., Zhang, S., Li, G. Y., & An, T. C. (2023). Pollution profiles, source identification and health risk assessment of heavy metals in soil near a non-ferrous metal smelting plant. *International Journal of Environmental Research and Public Health, 20*, 1004. https://doi.org/10.3390/ijerph20021004

Rao, K., Tang, T., Zhang, X., Wang, M., Liu, J. F., Wu, B., Wang, P., & Ma, Y. L. (2021). Spatial-temporal dynamics, ecological risk assessment, source identification and interactions with internal nutrients release of heavy metals in surface sediments from a large Chinese shallow lake. *Chemosphere, 282*, 131041. https://doi.org/10.1016/j.chemosphere.2021.131041

Rashid, A., Ayub, M., Ullah, Z., Ali, A., Sardar, T., Iqbal, J., Gao, X. B., Bundschuh, J., Li, C. C., Khattak, S. A., Ali, L., El-Serehy, H. A., Kaushik, P., & Khan, S. (2023). Groundwater quality, health risk assessment, and source distribution of heavy metals contamination around chromite mines: Application of GIS, Sustainable groundwater management, geostatistics, PCAMLR, and PMF receptor model. *International Journal of Environmental Research and Public Health, 20*, 2113. https://doi.org/10.3390/ijerph20032113

Rehman, I. U., Ishaq, M., Muhammad, S., Din, I. U., Khan, S., & Yaseen, M. (2020). Evaluation of arsenic contamination and potential risks assessment through water, soil and rice consumption. *Environ. Technol. Innovation, 20*, 101155. https://doi.org/10.1016/j.eti.2020.101155

Sakizadeh, M., & Zhang, C. S. (2021). Source identification and contribution of land uses to the observed values of heavy metals in soil samples of the border between the Northern Ireland and Republic of Ireland by receptor models and redundancy analysis. *Geoderma, 404*, 115313. https://doi.org/10.1016/j.geoderma.2021.115313

Sanga, V. F., Fabian, C., & Kimbokota, F. (2022). Heavy metal pollution in leachates and its impacts on the quality of groundwater resources around Iringa municipal solid waste dumpsite. *Environmental Science and Pollution Research, 30*, 8110–8122. https://doi.org/10.1007/s11356-022-22760-z

Sheng, D. R., Meng, X. H., Wen, X. H., Wu, J., Yu, H. J., & Wu, M. (2022). Contamination characteristics, source identification, and source-specific health risks of heavy metal(loid)s in groundwater of an arid oasis region in Northwest China. *Science of the Total Environment, 841*, 156733. https://doi.org/10.1016/j.scitotenv.2022.156733

Shi, H. H., Zeng, M., Peng, H. X., Huang, C. S., Sun, H. M., Hou, Q. Q., & Pi, P. C. (2022). Health risk assessment of heavy metals in groundwater of Hainan Island using the monte Carlo simulation coupled with the APCS/MLR model. *International Journal of Environmental Research and Public Health, 19*, 7827. https://doi.org/10.3390/ijerph19137827

Sun, J., Zhao, M., Huang, J., Liu, Y., Wu, Y., Cai, B., Han, Z., Huang, H., & Fan, Z. (2022). Determination of priority control factors for the management of soil trace metal(loid)s based on source-oriented health risk assessment. *Journal of Hazardous Materials, 423*, 127116. https://doi.org/10.1016/j.jhazmat.2021.127116

Wang, Q., Tian, Y. X., Wang, J., Li, J. Y., He, W. H., & Craig, N. J. (2023). Assessing pathways of heavy metal accumulation in aquaculture shrimp and their introductions into the pond environment based on a dynamic model and mass balance principle. *Science of the Total Environment, 881*, 163164. https://doi.org/10.1016/j.scitotenv.2023.163164

Wang, C., Wang, W. J., Shao, S. B., Deng, W. Q., Wang, C. Q., Liu, X. Y., Li, H. L., Wen, M. C., Zhang, X., Li, G. Y., & An, T. C. (2024). Occurrence of BTX and PAHs in underground drinking water of coking contaminated sites: Linkage with altitude and health risk assessment by boiling-modified models. *Science of the Total Environment, 917*, 170407. https://doi.org/10.1016/j.scitotenv.2024.170407

Wang, C. Q., Wang, W. J., Wang, C., Ren, S. X., Wu, Y. J., Wen, M. C., Li, G. Y., & An, T. C. (2025). Impact of coking plant to heavy metal characteristics in groundwater of surrounding areas: Spatial distribution, source apportionment and risk assessments. *Journal of Environmental Sciences, 149*, 688–698. https://doi.org/10.1016/j.jes.2024.01.048

Wu, Y. J., Qi, M. D., Yu, H., Li, G. Y., & An, T. C. (2025). Assessment of internal exposure risk from metals pollution of occupational and non-occupational populations around a non-ferrous metal smelting plant. *Journal of Environmental Sciences, 147*, 62–73. https://doi.org/10.1016/j.jes.2023.10.003

Xiang, Z. J., Wu, S. J., Zhu, L. Z., Yang, K., & Lin, D. H. (2024). Pollution characteristics and source apportionment of heavy metal(loid)s in soil and groundwater of a retired industrial park. *Journal of Environmental Sciences, 143*, 23–34. https://doi.org/10.1016/j.jes.2023.07.015

Yan, J. H., Chen, J. S., & Zhang, W. Q. (2023). A new probabilistic assessment process for human health risk (HHR) in groundwater with extensive fluoride and nitrate optimized by non parametric estimation method. *Water Research, 243*, 120379. https://doi.org/10.1016/j.watres.2023.120379

Zhang, W. J., Xin, C. L., & Yu, S. (2023). A Review of Heavy Metal Migration and Its Influencing Factors in Karst Groundwater. *Northern and Southern China. Water, 15*, 3690. https://doi.org/10.3390/w15203690

Zhang, K. F., Chang, S., Tu, X., Wang, E. R., Yu, Y. L., Liu, J. L., Wang, L., & Fu, Q. (2024a). Heavy metals in centralized drinking water sources of the Yangtze River: A comprehensive study from a basin-wide perspective. *Journal of Hazardous Materials, 469*, 133936. https://doi.org/10.1016/j.jhazmat.2024.133936

Zhang, K. F., Chang, S., Tu, X., Yu, Y. L., Shang, H. R., Wang, E. R., & Fu, Q. (2024b). A Comprehensive Study of Heavy Metals in Centralized Drinking Water Sources of the Yangtze River Basin: Levels, Sources, and

Probabilistic Health Risk. *Water, 16*, 3495. https://doi.org/10.3390/w16233495

Zhao, D., Wu, Q., Zeng, Y. F., Zhang, J., Mei, A. S., Zhang, X. H., Gao, S., Wang, H. Y., Liu, H. L., Zhang, Y., Qi, S., & Jia, X. (2023). Contamination and human health risk assessment of heavy metal(loid)s in topsoil and groundwater around mining and dressing factories in Chifeng, North China. *International Journal of Coal Science & Technology, 10*, 8. https://doi.org/10.1007/s40789-023-00568-7